Ultrafast Dynamics and Excited State Deactivation of $[Ru(bpy)_2Sq]^+$ and Its Derivatives

G. Ramakrishna,[†] D. Amilan Jose,[‡] D. Krishna Kumar,[‡] Amitava Das,*[,‡] Dipak K. Palit,[†] and Hirendra N. Ghosh*[,†]

Radiation & PhotoChemistry Division, Bhabha Atomic Research Centre, Mumbai 400085, India, and Central Salt and Marine Chemicals Research Institute, Bhavnagar 364002, Gujarat, India

Received: February 12, 2006; In Final Form: March 31, 2006

Femtosecond transient absorption spectroscopy has been employed to understand the excited state dynamics of $[Ru(bpy)_2Sq]^+$ (**I**; bpy is 2,2′-bipyridyl, and Sq is the deprotonated species of the semiquinone form of 1,2-dihydroxy benzene) and its derivatives, a widely studied near-infrared (NIR) active electrochromic dye. Apart from the well-defined $d\pi_{Ru} \rightarrow \pi^*_{bpy}$-based metal-to-ligand charge transfer (MLCT) transition bands at ∼480 nm, this class of molecules generally shows another $d\pi_{Ru} \rightarrow \pi^*_{Sq}$(SOMO)-based intense MLCT band at around 900 nm, which is known to be redox active and bleaches reversibly upon a change in the oxidation state of the coordinated dioxolene moiety. To have better insight into the photoinduced electron transfer dynamics associated with this MLCT transition, detailed investigations have been carried out on exciting this MLCT band at 800 nm. Immediately after photoexcitation, bleach at 900 nm has been observed, whose recovery is found to follow a triexponential function with major contribution from the ultrafast component. This ultrafast component of ∼220 fs has been ascribed to the S_1 to S_0 internal conversion process. In addition to the bleach, we have detected two transient species absorbing at 730 and 1000 nm with a formation time ∼220 fs for both species. The excited state lifetimes for these two transient species have been measured to be 1.5 and 11 ps and have been attributed to excited singlet (^{1}MLCT) and triplet (^{3}MLCT) states, respectively. Transient measurements carried out on the different but analogous derivatives (**II** and **III**) have also shown similar recovery dynamics except that the rate for the internal conversion process has increased with the decrease in the S_1 to S_0 energy gap. The observed results are consistent with the energy gap law for nonradiative decay from S_1 to S_0.

1. Introduction

Dye molecules, having strong absorption in the near-infrared (NIR) region of the spectrum, found applications in various fields such as optical data recording, photodynamic therapy, laser filters, and Q-switching of lasers.[1] Thus, recently, there has been growing interest for synthesizing the molecules, which have an absorption band with a high extinction coefficient in the NIR region and possess good stability.[2] Among various known NIR absorbing dyes such as polymethynes, Ni-dithiolenes, squaryllium, cyanine, multicomponent porphyrin derivatives, and some conducting polymers, Ru-dioxolene-based molecules have received significant attention over the past few years. Lever and co-workers[3] were the first to report the synthesis of $Ru(bpy)_2(Sq)^+$ (**I**; Chart 1) (bpy is 2,2′-bipyridyl, and Sq is the deprotonated species of the semiquinone form of 1,2-dihydroxy benzene), which shows an intense absorption band at 890 nm ($\epsilon_{890nm} = 6400\ mol^{-1}\ dm^3\ cm^{-1}$) due to the $Ru(d_\pi)(1b_2) \rightarrow Sq(^2b_2^*$, SOMO)-based metal-to-ligand charge transfer (MLCT) transition. Since then, several research groups have come up with reports on the synthesis of various derivatives of the Sq fragment of the $Ru(bpy)_2(Sq)^+$ in order to achieve a higher ϵ value for the NIR band. However, studies in this area are mostly restricted to the synthetic aspect of these molecules and studies on the electrochomic behavior.[3−6] The NIR band for these complexes is found to be redox active and bleaches reversibly upon a change in the oxidation state of the coordinated dioxolene fragment. This has provided Ru-dioxolene-based complexes an edge over some other NIR active dye molecules in their search for a reversible electrochromic NIR dye. Recently, Ward, Peter, and their co-workers anchored $Ru(dcbpy)_2(Sq^*)^+$ (dcbpy is 4,4′-dicarboxy-2,2′-bipyridine, and Sq* is substituted semiquinone derivative) molecules on nanocrystalline SnO_2 with an attempt to develop an efficient and realistic electrochromic device, which showed reversible elecrochromic behavior too.[4] No photoinduced interfacial electron transfer between nanocrystalline semiconductor (SnO_2) particle and $Ru(dcbpy)_2(sq)$ fragment was observed. It is strongly felt that, to design a practical optoelectronic device, it is almost essential to have insight into the dynamics of the excited state of this molecule, associated with the MLCT band in the NIR region. However, to date, no reports are available on studies of the photophysical properties or excited state dynamics of Ru-dioxolene-based complexes, barring a recent report on a preliminary photophysical investigation on a bichromophoric system derived from a Ru-dioxolene moiety.[7a] In our earlier work,[7b] we discussed in brief the ultrafast relaxation dynamics of **I** by excitation with a 400 nm femtosecond laser pulse. However, it will be interesting to monitor the ultrafast dynamics of **I** and its derivatives by selectively exciting the $d\pi_{Ru} \rightarrow \pi^*_{Sq}$(SOMO)-based MLCT band at 800 nm, where the excited state dynamics will not be complicated by the excitation of the $d\pi_{Ru} \rightarrow \pi^*_{bpy}$-based MLCT band. Excited state dynamics for the MLCT band of a closely related complex, $Ru(bpy)_3^{2+}$ (λ_{max}: $d\pi_{Ru} \rightarrow \pi^*_{bpy} = 450$ nm) has been

* To whom correspondence should be addressed. E-mail: hnghosh@magnum.barc.ernet.in (H.N.G); amitava@csmcri.org (A.D.). Fax: 00-91-22-2550-5151 (H.N.G.).

[†] Bhabha Atomic Research Centre.

[‡] Central Salt and Marine Chemicals Research Institute.

10.1021/jp060906c CCC: $33.50
Published on Web 05/03/2006

CHART 1: Molecular Structures of Ru-dioxolene Complexes Investigated in the Present Work

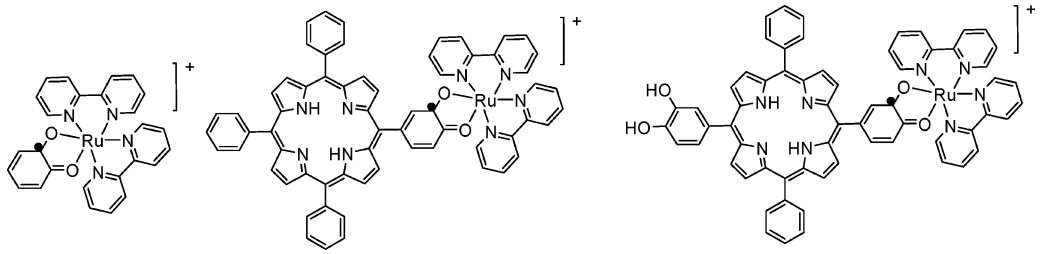

Ru-Sq (**I**) TPP-Ru-Sq (**II**) Cat TPP-Ru-Sq (**III**)

pursued with intense research interest in recent years.[8,9] Ultrafast pump−probe spectroscopic studies on **I** after excitation at 800 nm at the $d\pi_{Ru} \rightarrow \pi^*_{Sq}$(SOMO)-based MLCT transition band are expected to reveal information on the excited state dynamics associated with this transition. Further, NIR absorbing dyes have a small energy difference between the ground and excited states and study on these molecules will be of immense help in understanding the energy gap law.[10−12]

In the present investigation, we have addressed the two key issues through time-resolved absorption studies in the femtosecond time domain on **I** and two other closely related derivatives (**II** and **III**, Chart 1) with varying energy for the MLCT transition in the NIR region. The complicated excited state decay dynamics has been explained with the involvement of two transient states, namely, excited singlet (^{1}MLCT) and triplet (^{3}MLCT) states. Interesting observation of S_1-S_0 internal conversion has been made, whose rate increases with decreasing energy gap, thus providing evidence for the energy gap law.

2. Experimental Section

(a) Materials. Complexes **I**, **II**, and **III** were synthesized following known literature procedures and were characterized by various standard analytical and spectroscopic methods.[3a,7,13,14] Analytical and spectroscopic data are in good agreement with that for proposed formulation for these complexes. All reactions were performed under an argon atmosphere unless stated otherwise. The water used was doubly distilled. All other chemicals were obtained locally and were used as such without further purification. The acetonitrile, methanol, dichloromethane, and 2-propanol used were of spectroscopic grade and were used as such. Optical absorption measurements have been carried out with a Shimadzu UV−vis−NIR 3101 PC spectrophotometer. A Hitachi F 4100 fluorescence spectrometer has been used to study the luminescence from the samples. All spectral and photophysical measurements were carried out in the solution, thoroughly purged with dinitrogen gas.

(b) Femtosecond Transient Absorption Spectrometer. The femtosecond tunable visible spectrometer has been developed on the basis of a multipass amplified femtosecond Ti:sapphire laser system from CDP-Avesta, Russia (1 kHz repetition rate at 800 nm, 50 fs, 200 μJ/pulse), and has been described earlier.[15] The 800 nm output pulses from the multipass amplifier are split into two parts to generate pump and probe pulses. One part of it is used to excite the sample. To generate visible probe pulses, about 2 μJ of the 800 nm beam is focused onto a 1.5 mm thick sapphire window. The intensity of the 800 nm beam is adjusted by iris size and ND filters to obtain a stable white light continuum in the 400 nm to over 1000 nm region. The probe pulses are split into the signal and reference beams and are detected by two matched photodiodes with variable gain. We have kept the spot sizes of the pump beam and probe beam at the crossing point around 500 and 300 μm, respectively. The excitation energy density (at 400 nm) was adjusted to ~2500 μJ/cm^2. The noise level of the white light is about ~0.5% with occasional spikes due to oscillator fluctuation. We have noticed that most laser noise is low-frequency noise and can be eliminated by comparing the adjacent probe laser pulses (pump blocked vs unblocked using a mechanical chopper). The typical noise in the measured absorbance change is about <0.3%. The instrument response function was obtained by fitting the rise time of the bleach of sodium salt of *meso* tetrakis (4-sulfonatophenyl) porphyrin (TPPS) at 710 nm, which has an instantaneous response. The fundamental from the Ti:sapphire has been used to excite the sample. We have determined the instrument response function, and it is found to be 95 fs for an 800 nm excitation pulse.

3. Results

UV−vis−NIR spectra were recorded for complexes **I**, **II**, and **III** in CH_3CN are shown in Figure 1. All of these complexes show characteristic $d\pi_{Ru} \rightarrow \pi^*_{Sq}$(SOMO)-based MLCT in the NIR region of the spectrum, and the λ_{max} values for this absorption band are summarized in Table 1. A gradual shift in λ_{max} for the $d\pi_{Ru} \rightarrow \pi^*_{Sq}$-based MLCT band toward longer wavelength is observed for complexes **I**−**III**. Otherwise, spectra for **II** and **III** in the UV−vis region are dominated by the spectral features of the porphyrin fragment.

To have better insight into the excited state deactivation processes associated with $d\pi_{Ru} \rightarrow \pi^*_{Sq}$(SOMO)-based MLCT

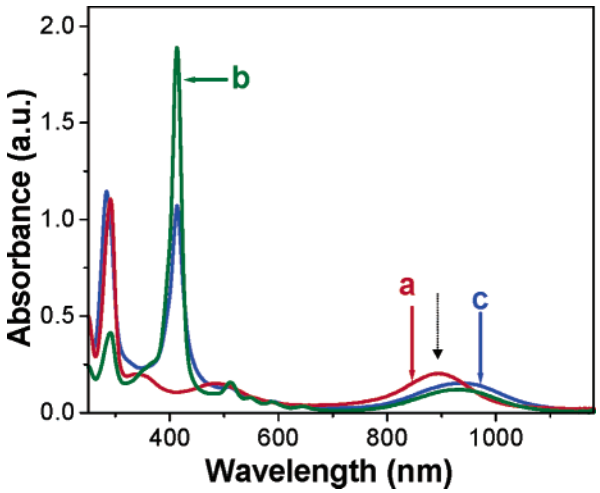

Figure 1. Optical absorption spectrum of **I** (a, 3.2 × 10^{-5} mol dm^{-3}), **II** (b, 2.9 × 10^{-6} mol dm^{-3}), and **III** (c, 3.0 × 10^{-6} mol dm^{-3}) in acetonitrile. The arrow indicates the λ_{max} value for the $d\pi_{Ru} \rightarrow \pi^*_{Sq}$(SOMO)-based transition for **I**.

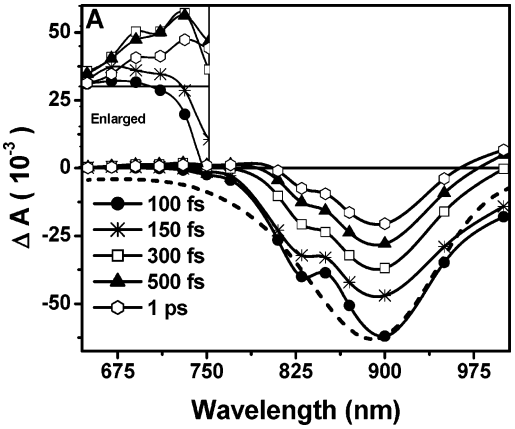

Figure 2. Time-resolved transient absorption spectrum of **I** in acetonitrile at various time delays after excitation at 800 nm. The spectrum at each time delay consists of a bleach with a maximum centered around 900 nm with a shoulder at 830 nm. Also, a positive transient absorption has been observed at 730 nm (inset A, expanded) and another at 1000 nm.

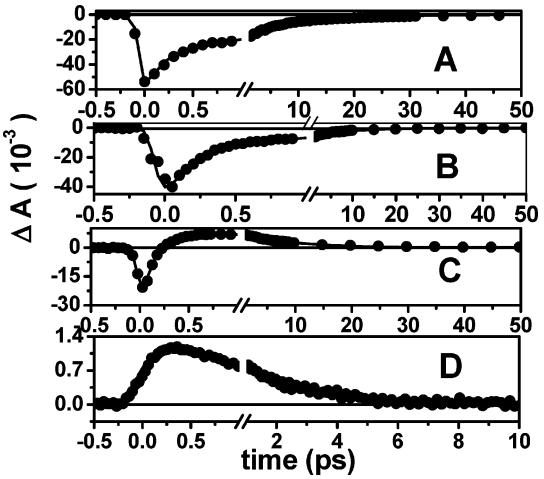

Figure 3. Kinetic decay traces of **I** in acetonitrile at different probe wavelengths after excitation with an 800 nm laser pulse: (A) 900 nm; (B) 830 nm; (C) 730 nm; (D) 1000 nm.

TABLE 1: Optical Absorption Maxima for the $d\pi_{Ru} \rightarrow \pi^*_{Sq}$(SOMO) Transition Band and E_g (in eV) Values for I, II, and III in Acetonitrile

compound	λ_{max} (nm)	E_g (eV)
I	890	1.40
II	930	1.34
II	960	1.29

transition in **I**−**III**, transients of the respective excited states in real time have been monitored using femtosecond pump−probe spectroscopy after exciting this band at 800 nm using a Ti:sapphire laser. A transient absorption spectrum of **I** in acetonitrile at various time delays is shown in Figure 2. The spectrum, at each time delay, consists of bleach in the 770−1000 nm region centered at 900 nm and a minor growth in absorption bands at around 730 and 1000 nm. The dynamics of the transient absorption bands at representative wavelengths, that is, at 900, 730, 830, and 1000 nm, are shown in Figure 3. Kinetic traces follow a multiexponential function, and different time constant values are provided in Table 2. This clearly shows that the decay of the excited state is fast and follows a multiexponential function. Thus, the associated dynamics is not straightforward and involves a greater number of states. To confirm whether the observed complicated dynamics is the signature of $d\pi_{Ru} \rightarrow \pi^*_{Sq}$(SOMO) transition or not, investigations have been extended to two analogous derivatives (**II** and **III**). Similar multiexponential recovery has been observed for the other two derivatives too, but with different time constants (Figure 4; Table 3). Solvent dependent experiments have also been carried out; the bleach recovery kinetics followed for **I** in different solvents of varying thermal diffusivity have been shown in Figure 5 and the time constants are summarized in Table 4. Interestingly, all the kinetics in different solvents are found to be more or less similar. The dynamics followed for different derivatives has shown an interesting trend, in which the ultrafast lifetime became much faster with decreasing energy gap of S_1 to S_0.

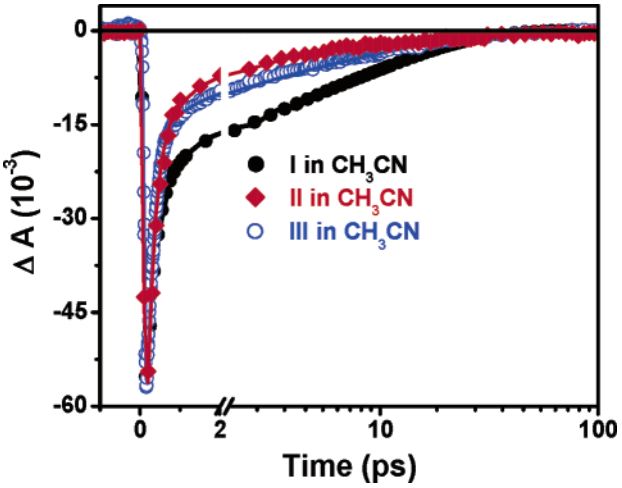

Figure 4. Kinetics of bleach recovery for **I**, **II**, and **III** in acetonitrile, monitored at their respective bleach maxima.

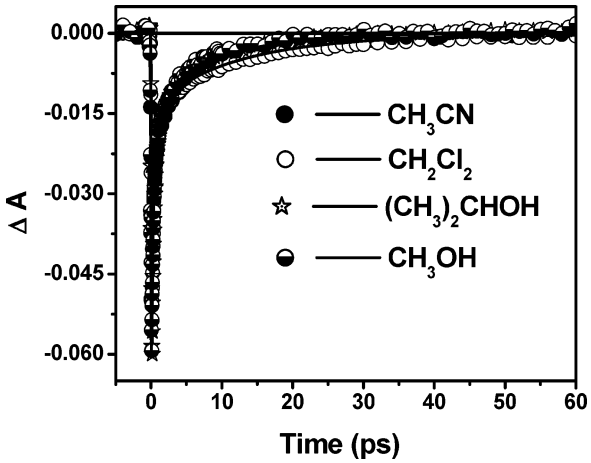

Figure 5. Bleach recovery dynamics of **I** at 900 nm monitored in different solvents.

TABLE 2: Lifetimes of I in Acetonitrile at Different Wavelengths

λ (nm)	lifetimes
900	$\tau_1 = 220$ fs (60%), $\tau_2 = 1.5$ ps (20%), $\tau_3 = 11$ ps (20%)
730	$\tau_1 = 220$ fs (−100%), $\tau_2 = 1.5$ ps (100%)
830	$\tau_1 = 200$ fs (86%), $\tau_2 = 1.5$ ps (7%), $\tau_3 = 11$ ps (7%)
1000	$\tau_1 = 200$ fs (−145%), $\tau_2 = 11$ ps (100%)

4. Discussion

(a) Characterization of Optical Transitions. To comprehend the results presented in the previous section, it is necessary to characterize the transitions involved in the complex in its optical ground state. In most cases of polypyridyl complexes of ruthenium(II) (RuL_3^{2+}, where L is 2,2′-bipyridyl or its

TABLE 3: Bleach Recovery Dynamics of I and Its Derivatives at Respective Bleach Maxima

dye	lifetimes	$\langle\tau_{av}\rangle$ (ps)
I	$\tau_1 = 0.22 \pm 0.03$ ps (59.7%), $\tau_2 = 1.5 \pm 0.2$ ps (20.2%), $\tau_3 = 11 \pm 0.5$ ps (20.1%)	2.63
II	$\tau_1 = 0.20 \pm 0.03$ ps (80.3%), $\tau_2 = 1.6 \pm 0.2$ ps (15.7%), $\tau_3 = 28 \pm 1$ ps (4%)	1.53
III	$\tau_1 = 0.18 \pm 0.03$ ps (78%), $\tau_2 = 1.6 \pm 0.2$ ps (11%), $\tau_3 = 10 \pm 0.5$ ps (11%)	1.42

TABLE 4: Bleach Recovery Lifetimes of I in Various Media Monitored at 900 nm

solvent	lifetimes
CH_3CN	$\tau_1 = 0.22 \pm 0.03$ ps (59.7%), $\tau_2 = 1.5 \pm 0.2$ ps (20.2%), $\tau_3 = 11 \pm 0.5$ ps (20.1%)
CH_2Cl_2	$\tau_1 = 0.22 \pm 0.03$ ps (66.7%), $\tau_2 = 1.5 \pm 0.2$ ps (15.6%), $\tau_3 = 12.5 \pm 0.5$ ps (17.3%)
$(CH_3)_2CHOH$	$\tau_1 = 0.22 \pm 0.03$ ps (66.7%), $\tau_2 = 1.5 \pm 0.2$ ps (20.8%), $\tau_3 = 11 \pm 0.5$ ps (12.5%)
CH_3OH	$\tau_1 = 0.22 \pm 0.03$ ps (66.7%), $\tau_2 = 1.5 \pm 0.2$ ps (20.5%), $\tau_3 = 11 \pm 0.5$ ps (12.8%)

derivatives), the optical absorption spectrum is principally dominated by the presence of $d\pi_{Ru}$ to π^*_L-based MLCT transition at around 450 nm along with some ligand based ($\pi-\pi^*$) transitions in the UV region. Lever and others have made assignments of the absorption bands in the optical spectrum recorded for **I** and related complexes,[3] and the assignments of the important spectral features are as follows: the strong absorption band ($\epsilon = 6400$ dm^3 mol^{-1} cm^{-1}) for **I** in the NIR region has been attributed to a MLCT transition associated with an electronic transition from the $d\pi_{Ru}(^1b_2)$ orbital to a ligand centered SOMO of Sq($^2b_2$*), the broad absorption band with a maximum at around 480 nm and with an extinction coefficient of 2500 dm^3 mol^{-1} cm^{-1} is assigned to $d\pi_{Ru} \rightarrow \pi^*_{bpy}$-based transition, and the other bands in the UV region are attributed to ligand centered $\pi-\pi^*$ and n$-\pi^*$ transitions. The essence of absorption measurements is that the molecule is having two MLCT bands involving two different coordinated ligands—one of them is bpy and another is Sq. Similar MLCT bands in the NIR region are observed for the derivatives **II** and **III** (Table 1). It is interesting to note that, as the substituent is changed from H to porphyrin to porphyrin-cat, a gradual shift toward the longer wavelengths for the NIR band has been observed, which is very much consistent with the earlier results.[6,7]

(b) Excited State Deactivation. The electron transfer dynamics, associated with the $d\pi_{Ru} \rightarrow \pi^*_{bpy}$-based MLCT band around 450 nm, for RuL_3^{2+} complexes is extensively studied by various research groups in the nano-/pico-/femtosecond time domain and is well understood.[8] For complexes **I**−**III**, an instant bleach (Figure 2) is observed—centered around 900 nm—when excited at 800 nm and kinetic traces at different probe wavelengths such as 730, 830, 900, and 1000 nm are presented in Figure 3. Electrochemical studies have clearly shown that the reduction potential for the Sq/Sq$^-$ process is favored over the bpy/bpy$^-$-based processes by ~1.0 V. This signifies that the SOMO for Sq-based ligands is considerably lower in energy compared with the LUMO for the bpy ligand. Thus, it is expected that, upon excitation of **I** at 800 nm laser light, photoexcited electrons get localized on coordinated semiquinone fragments which results in the formation of the corresponding reduced dioxolene species with anticipated bleaching of the absorption band in the NIR region (Figure 2). This agrees well with the earlier reports of the spectroelectrochemical studies on **I** and other related complexes by various groups, including some from this group.[3−7] Spectroelectrochemical studies have shown that the band at 890 nm bleaches completely upon reduction to the corresponding catechol fragment and reappears with the original intensity upon reversal of the redox process.[3−7]

Recovery of the bleach (Figure 2) was found to be fast, and kinetic studies (Figure 3) are expected to provide information on the excited state decay dynamics of the molecule as it populates back the ground state. Accordingly, the bleach recovery dynamics at 900 nm is followed and is shown in Figure 3A. The bleach recovers very fast and a major fraction is recovered within a 1 ps time scale. The kinetic recovery trace has been best fitted with a multiexponential function with time constants of 220 ± 30 fs (60%), 1.5 ± 0.2 ps (20%), and 11 ± 0.5 ps (20%) (Table 2). It is interesting to note that, in the transient absorption spectra, a new spectral feature appears at around 830 nm. We have monitored the recovery kinetics at 830 nm (Figure 3B). The kinetic trace at 830 nm is best fitted with time constants of 200 fs (86%), 1.5 ps (7%), and 11 ps (7%) (Table 2). Thus, bleach recovery kinetics at 830 nm also have similar time constants with different pre-exponential components. The difference in the pre-exponents can be attributed to the positive absorption of the excited states at that wavelength. Even the feature in the bleach might also be due to the excited state absorption at that particular wavelength region.

The earlier works on ultrafast transient measurements of a related complex, $Ru(bpy)_3^{2+}$, suggest that the bleach corresponding to the MLCT state ($d\pi_{Ru} \rightarrow \pi^*_{bpy}$) does not recover within 500 ps (maximum delay time one can get with the instrument used for this study), as the intersystem crossing (ISC) to the triplet state does happen with unit quantum yield.[8] However, the fluorescence up conversion and transient absorption measurements carried out on $Ru(bpy)_3^{2+}$-based complexes suggest that the ISC rate is in the order of 40 fs[9] and the triplet state is populated within 300 fs.[8a] The results also suggest a cascade relaxation of the singlet state, which competes with processes such as ISC and internal conversion (IC).[8a,b,9] Bleach observed in the present investigation with complex **I** does recover very fast and is completed within 50 ps. This result is rather striking, at least when compared with that of $Ru(bpy)_3^{2+}$. However, it is understandable if one considers the fact that the molecular orbitals involved in the two different MLCT transitions are different for two complexes and hence the deactivation processes. On the other hand, this can be addressed by following the dynamics of excited state absorption (ESA), observed in the transient absorption spectrum. The kinetic trace of the transient observed at 730 nm is shown in Figure 3C. It is interesting to note that there is a slower growth, which subsequently decays back to the ground state within 11 ps. The trace has been best fitted with a growth time constant of 200 ± 30 fs and a decay time constant of 1.5 ± 0.2 ps. These results reveal that one excited state is formed with a time constant, which is almost similar to the decay of the singlet state (observed from the bleach recovery dynamics, 220 fs component). The state that has grown eventually decays back to the ground state with a time constant of 1.5 ps, which is also reflected in the bleach recovery dynamics. Further, the kinetic trace of the transient observed at 1000 nm is shown in Figure 3D. This shows instantaneous bleach followed by growth to give transient absorption within 1 ps, which is eventually decayed within 50 ps. The trace has been best fitted with a multiexponential

SCHEME 1: Mechanistic Scheme Showing the Excited State Dynamics of I after Excitation at 800 nm[a]

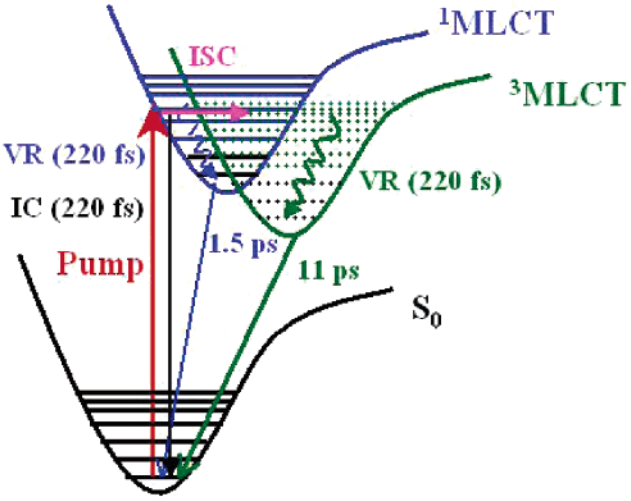

[a] ^{1}MLCT and ^{3}MLCT are the excited singlet and triplet states.

function with one time constant referring to the instantaneous bleach, a growth component of 220 ± 30 fs and a decay component of 11 ± 0.5 ps. Similar to the kinetics at 730 nm, the two time constants obtained at 1000 nm match well with the bleach recovery dynamics at 900 nm (Figure 3A). Here again, the observation can be explained on the basis of the formation of one more state with a time constant of 220 fs which decays back to the ground state within 11 ps. Thus, kinetic traces at different wavelengths indicate the presence of two different excited states.

The excited state dynamics of complex **I** can be explained clearly by adopting Scheme 1. As we have already observed, the excited state of complex **I** comes back to the ground state after following some complicated path. If we follow Scheme 1, upon excitation, the molecule gets excited to the S_1 state, which is vibrationally hot. We have designated the S_1 state as the ^{1}MLCT state. Now this hot ^{1}MLCT state can relax down to the ground state through very fast internal conversion with a time constant of 220 fs. This kinetic path contributed 60% of the total de-excitation process, which can be seen in Table 2. This has been determined after monitoring the bleach recovery kinetics at 900 nm. The rest of the 40% of the hot ^{1}MLCT states can be de-excited by the following ways. The energy level of the ^{1}MLCT state is very low, and these energy levels are expected to overlap with the vibrationally hot ^{3}MLCT state. Bhasikuttan et al.[9] reported that the intersystem crossing (ISC) process can be as fast as <40 fs or faster for vibrational relaxation from the ^{1}MLCT state to the ^{3}MLCT state in the case of $Ru(bpy)_3^{2+}$. When the vibrational energy levels of the hot ^{1}MLCT state overlap with the upper vibrational energy levels of the ^{3}MLCT states, the ISC process can be very fast (within the pulse in our present laser system) with the formation of hot ^{3}MLCT states. Now in the present investigation, two transients at 730 and 1000 nm can be attributed to the ^{1}MLCT and ^{3}MLCT states, respectively. We have observed a growth time for both transients of ~220 fs (Table 2), which we have attributed to the vibration relaxation for the singlet (^{1}MLCT) and triplet ^{3}MLCT) states. We have observed that the transient species at 730 nm follow a single exponential decay pathway with a time constant of 1.5 ps, which we can attribute to the lifetime of the ^{1}MLCT state. On the other hand, the transient species at 1000 nm also decay single exponentially with a time constant of 11 ps, which can be attributed to the lifetime of the ^{3}MLCT state. Interestingly, the excited state lifetime of the ^{1}MLCT and ^{3}MLCT states matches exactly with the bleach recovery kinetics at 900 nm (Table 2).

However, we cannot rule out the vibrationally excited states of the S_0 state. If they are the vibrationally hot states of the ground state corresponding to the two different vibrational modes of the two stretching modes of Ru−O bonds, then they will vibrationally relax to give the ground state. If the two components are for vibrational cooling, it is desirable for one to see the effect of thermal diffusivity of the solvent on the vibrational cooling dynamics. For this reason, we have carried out the excited state dynamics of **I** in several solvents of different thermal diffusivities such as dichloromethane, methanol, and 2-propanol. Interestingly, we have observed similar decay components for all of the solvents (Figure 5 and Table 4). This solvent independent nature of the dynamics can rule out the possibility of vibrational cooling of the excited state. Hence, we attribute these states to two different electronic excited states, namely, the excited singlet (^{1}MLCT) and triplet (^{3}MLCT) states (Scheme 1).

In this context, we would like to compare the ultrafast dynamics of **I** after excitation at 400 nm which we have reported earlier.[7b] Upon exciting **I** at 800 nm, we could selectively excite only the $d\pi_{Ru} \rightarrow \pi^*_{Sq}$(SOMO)-based MLCT bands, while excitation at 400 nm caused the excitation of both the $d\pi_{Ru} \rightarrow \pi^*_{bpy}$ and $d\pi_{Ru} \rightarrow \pi^*_{Sq}$-based MLCT bands.[7b] The transient spectra observed in these two cases looked different. After excitation with a 400 nm laser pulse, time-resolved spectra at different time delays show positive absorbance in the spectral range 520−760 nm along with big bleach at around 900 nm.[7b] The transient peaks, in the wavelength range 520−760 nm, have been attributed to the excited state absorption of the $d\pi_{Ru} \rightarrow \pi^*_{bpy}$-based MLCT transition. Bleach at 900 nm recovers by 50 ps, and at a longer time scale, it shows a positive absorption, which has been attributed to the excited state absorption of the $d\pi_{Ru} \rightarrow \pi^*_{bpy}$-based ^{3}MLCT state. When excited at 800 nm, the time-resolved absorption spectrum shows a very weak absorption in the 700 nm region and bleach at 900 nm recovers within less than 100 ps. However, we feel that the bleach recovery kinetics at 900 nm does not change much at different excitation wavelengths. The faster decay components are very similar.

In the present investigation, as we are discussing the ultrafast component of ~200 fs, it is expected that solvation dynamics[16,17] may play a major role in the excited state dynamics in these systems. Here, we have monitored the excited state dynamics in acetonitrile where $\langle\tau_s\rangle$ (average solvation time) varies from 480 to 600 fs[18] and again it can vary from solvent to solvent. The solvation dynamics[18] is slower (6−10 ps) in methanol and much slower (~30 ps) in propanol as compared with that in acetonitrile (480−600 fs). However, the bleach recovery kinetics of **I**, as depicted in Figure 5 and Table 4, clearly indicates that it does not change from propanol to methanol to acetonitrile. If solvent dynamics played a major role, then we would have observed different dynamics in different solvents for these systems. Again, optical absorption measurements of **I** confirmed that the absorption peak in solutions of different polarities does not change much from low-polarity solvents like hexane to high-polarity solvents like acetonitrile.[6d] This clearly indicates these molecules are not polar in nature, and as a result, there will not be much of an effect of solvent (solvation dynamics) in the excited state dynamics. However, there may be little effect of solvation dynamics on the excited dynamics of these molecules and it may be very negligible in these systems.

(c) Excited State Dynamics of the Derivatives. The observation of multiexponential recovery dynamics is rather unique and not normally observed for simple molecules. Thus, it is almost essential to ascertain whether this recovery dynamics involves only the noninnocent ligand (Sq). To address this issue and to understand the dynamics of the other derivatives (**II** and **III**), transient absorption measurements on **II** and **III** have been carried out following excitation at 800 nm. Figure 4 shows the dynamics of bleach recovery of **I**, **II**, and **III** at their respective bleach maxima, and the corresponding time constants are summarized in Table 3. It is interesting to note that the dynamics of the bleach recovery for **II** and **III** are multiexponential with three time constants similar to that of **I**. These results suggest that it is indeed the noninnocent Sq fragment which is actually governing the recovery dynamics and is independent of the environment or any other factor. A close look at the time constants presented in Table 3 suggests an interesting observation. With some sort of increase in conjugation of the Sq fragment, the faster component of the decay dynamics became much faster, whose origin has been emphasized in the following section.

(d) Energy Gap Law for Internal Conversion. The observed ultrafast component of 220 fs in the bleach recovery kinetics of **I** indicates that the singlet lifetime is very short, which is not normally observed in organic or inorganic molecules. This cannot be attributed to any conformational relaxation of the S_1 state to give the S_0 state, as the molecule is rigid. The dynamics can be attributed to the $S_1 \rightarrow S_0$ IC process through a nonradiative pathway, and this is possible when there is a coupling of the vibronic energy levels of the S_1 state to the isoenergetic vibrational levels of the ground state. Conventionally, chemist's intuition tells us that the $S_1 \rightarrow S_0$ IC is inefficient, with typical time constants of nano- to microseconds.[12] However, in recent years, several molecules (DNA and RNA nucleosides,[19] spiropyran and merocyanine dyes,[20] etc.) have been found to show faster $S_1 \rightarrow S_0$ internal conversion rates even up to the femtosecond range.

According to the energy gap law,[10,12] the rate of internal conversion (k_{IC}) for electronic transition can be expressed as $k_{IC} \sim 10^{13} f_v$ and $k_{IC} \sim 10^{13} \exp(-\alpha \Delta E)$, where f_v is a sensitive function of the energy gap (ΔE), the energy difference between S_1 and S_0, and α is the proportionality constant. Meyer and coworkers[11] have established the validity of the energy gap law, and it was found that the $\ln(k_{IC})$ values varied linearly with ΔE for a given type of molecules and slopes are found to be different for a different set of molecules. The ultrafast component observed in the present investigation is ascribed to the IC rate from $S_1 \rightarrow S_0$. If this has to be true, we should be able to see a behavior similar to that of the energy gap law. It is interesting to see from Table 3 that the ultrafast time constant has decreased with decreasing energy gap between S_1 and S_0. The plot of $\ln(k_{IC})$ versus energy gap is shown in Figure 6. The noteworthy outcome is that the observed IC process to a major extent validates the energy gap law. Although we have only compared the time constants for the fastest decay component (nonradiative decay) with the energy gap law for all three complexes, we can show that the energy gap law still can be valid if we take the average time constant to reach the ground state (Table 3).

Moreover, McCusker and co-workers have also shown that, apart from ΔE, k_{IC} also depends on the internuclear distance (ΔQ) in the excited state.[8c] In the present investigation, ΔE is about 1.34 eV, which is much less, and hence, by following the energy gap law, we can attribute the 220 fs component to the IC process from S_1 to S_0.

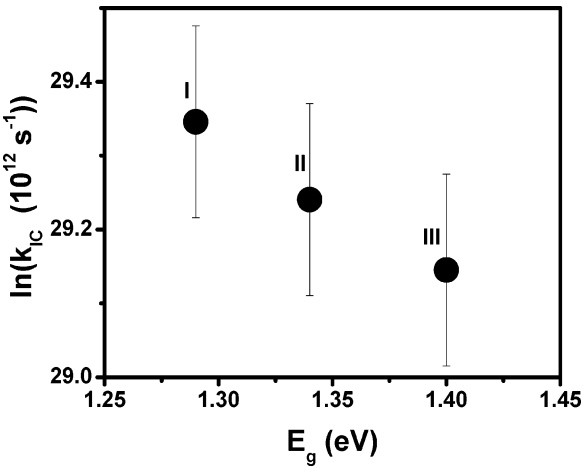

Figure 6. Plot of the rate of internal conversion of S_1-S_0 with the energy gap.

5. Conclusion

In a nutshell, the presented paper describes the excited state deactivation of the NIR band of the primary unit in Ru-dioxolene complexes, that is, **I**, **II**, and **III**. Ultrafast transient measurements with excitation at 800 nm have been carried out on **I**, **II**, and **III** to reveal the excited state dynamics. Upon excitation at 800 nm, the MLCT band corresponding to the $d\pi_{Ru}$ ($^1b_1$) $\rightarrow$ $SOMO_{Sq}$ ($^2b_2$*) transition is populated and is responsible for a bleach centered at 900 nm in the difference spectrum. The bleach recovery dynamics gives the information on excited state deactivation, which is found to follow a triexponential with typical lifetimes of 220 fs (60%), 1.5 ps (20%), and 11 ps (20%). The multiexponential recovery dynamics have shown that the excited state does involve a greater number of states. The presence of two other electronic excited states in the decay dynamics is confirmed by the observation of two excited state absorption bands with single exponential lifetimes of 1.5 and 11 ps. We have attributed these two transient species to excited singlet (^{1}MLCT) and triplet (^{3}MLCT) states, respectively. The growth of these excited species has been attributed to the vibrational relaxation times of the ^{1}MLCT and ^{3}MLCT states. The 220 fs component in the bleach recovery kinetics has been ascribed to S_1-S_0 internal conversion. Transient absorption studies on **II** and **III** have also shown a similar multiexponential bleach recovery as that of **I**, suggesting that the noninnocent ligand of Sq attached to the Ru-metal center is controlling the excited state deactivation. The ultrafast IC rate has indeed followed the well-established energy gap law. This light fastness of the NIR band of the Ru−Sq molecule and its derivatives can be made useful for applications of these molecules as NIR sensors for optoelectronic devices, laser filters, and Q-switching of lasers.

Acknowledgment. H.N.G. and A.D. acknowledge Dr. T. Mukherjee (Director, Chemistry Group, BARC, Mumbai), Dr. S. K. Sarkar (Head, RPC Division), and Dr. P. K. Ghosh (Director, CSMCRI, Bhavnagar) for their keen interest in this work. Board of Research in Nuclear Science (BRNS) and Department of Science and Technology (DST), Government of India, support this work. D.A.J. and D.K.K. acknowledge CSIR for Sr. Research Fellowship.

References and Notes

(1) For an introduction, see: (a) Rosseinsky, D. R.; Mortimer, R. J. *Adv. Mater*. **2001**, *13*, 783. (b) Mortimer, R. J. *Chem. Soc. Rev.* **1997**, *26*,

147. (c) Blake, L. M.; Rees, L. H.; Claridge, T. D. W.; Anderson, H. L. *Angew. Chem., Int. Ed. Engl.* **2000**, *39*, 818.

(2) (a) Fabian, J.; Nakazumi, H.; Matsuoka, M. *Chem. Rev.* **1992**, *92*, 1197 and references therein. (b) Emmelius, M.; Pawlowski, G.; Vollman, H. W. *Angew. Chem., Int. Ed. Engl.* **1989**, *28*, 1445. (c) Tsuda, A.; Osuka, A. *Science* **2001**, *293*, 79. (d) Shukla, A. D.; Bajaj, H. C.; Das, A. *Angew. Chem., Int. Ed. Engl.* **2001**, *40*, 1446. (e) Drobizhev, M.; Stepanenko, Y.; Dzenis, Y.; Karotki, A.; Rebane, A.; Taylor, P. N.; Anderson, H. L. *J. Phys. Chem. B* **2005**, *109*, 7233.

(3) (a) Haga, M.; Dodsworth, E. S.; Lever, A. B. P. *Inorg. Chem.* **1986**, *25*, 447. (b) Lever, A. B. P.; Masui, H.; Metcalfe, R. A.; Stufkens, D. H.; Dodsworth, E. S.; Auburn, P. R. *Coord. Chem. Rev.* **1993**, *125*, 317. (c) Masui, H.; Lever, A. B. P.; Auburn, P. R. *Inorg. Chem.* **1991**, *30*, 2402.

(4) Cañadas, J. G.; Meacham, A. P.; Peter, L. M.; Ward, M. D. *Angew. Chem., Int. Ed. Engl.* **2003**, *42*, 3011.

(5) (a) Bartham, A. M.; Cleary, R. L.; Kowallick, R.; Ward, M. D. *Chem. Commun.* **1998**, 2695. (b) Schwab, P. F. H.; Diegoli, S.; Biancardo, M.; Bignozzi, C. A. *Inorg. Chem.* **2003**, *42*, 6613.

(6) (a) Shukla, A. D.; Das, A. *Polyhedron* **2000**, *19*, 2605. (b) Ghosh, D.; Shukla, A. D.; Banerjee, R.; Das, A. *J. Chem. Soc., Dalton Trans.* **2001**, 1 and references therein. (c) Shukla, A. D.; Whittle, B.; Bajaj, H. C.; Das, A.; Ward, M. D. *Inorg. Chim. Acta* **1999**, *285*, 89. (d) Ghosh, D.; Shukla, A. D.; Banerjee, R.; Das, A. *J. Chem. Soc., Dalton Trans.* **2002**, 1220. (e) Ward, M. D.; McCleverty, J. A. *J. Chem. Soc., Dalton Trans*. **2002**, 275 and references therein.

(7) (a) Shukla, A. D.; Ganguly, B.; Dave, P. C.; Samanta, A.; Das, A. *Chem. Commun*. **2002**, *22*, 2648. (b) Jose, A. D.; Kumar, D. K.; Das, A.; Ramakrishna, G.; Palit, D. K.; Ghosh, H. N. *Inorg. Chem.* **2005**, *44*, 2414.

(8) (a) Damrauer, N. H.; Cerullo, G.; Yeh, A.; Boussir, T. R.; Shank, C. V.; McCusker, J. K. *Science* **1997**, *275*, 54. (b) Yeh, A. T.; Shank, C. V.; McCusker, J. K. *Science* **2000**, *289*, 935. (c) McCusker, J. K. *Acc. Chem. Res.* **2003**, *36*, 876 and references therein.

(9) Bhasikuttan, A. C.; Suzuki, M.; Nakashima, S.; Okada, T. *J. Am. Chem. Soc.* **2002**, *124*, 8398.

(10) Siebrand, W. J. *J. Chem. Phys.* **1966**, *44*, 4055.

(11) (a) Caspar, J. V.; Meyer, T. J. *J. Phys. Chem.* **1983**, *87*, 952. (b) Treadway, J. A.; Leob, B.; Lopez, R.; Anderson, P. A.; Keene, F. R.; Meyer, T. J. *Inorg. Chem.* **1996**, *35*, 2242. (c) Chen, P.; Meyer. T. J. *Chem. Rev.* **1998**, *98*, 14 and references therein.

(12) Turro, N. J. *Modern Molecular Photochemistry*; The Benzmin/Cummings Publishing Co., Inc: Menlo Park, CA, 1978.

(13) The complex has been synthesized by reaction of $[Ru(bp)_2Cl_2]\cdot 2H_2O$ (0.156 g, 0.3 mmol) with appropriate dioxolene ligands—3,4-dihydroxy benzene (0.035 g, 0.31 mM) for complex **I**; 1-(3,4-dihydroxy phenyl)-5,10,15-triphenyl porphyrin (0.2 g, 0.31 mM) for complex **II**, and bis-1,10-(3,4-dihydroxy phenyl)-5,15-bis phenyl porphyrin (0.21 g, 0.31 mM) for complex **III**—in ~50 mL of an ethanol—water mixture at refluxing temperature for 6 h. Then, the reaction mixture was allowed to cool to room temperature and was stirred at room temperature with an equivalent amount of ferrocenium salt ($FcPF_6$) to ascertain the complete conversion to the semiquinone form. After that, ethanol was removed under vacuum and the desired complexes were precipitated as brown solid by adding an excess of aqueous KPF_6 or NH_4PF_6 solution. This was filtered off, washed with cold water, and air-dried. The crude product in each case was purified by gravity chromatography on silica (as the stationary phase) and using CH_3CN-saturated aqueous NH_4PF_6 solution (98:2, v/v) as the eluent. CH_3CN was removed under vacuum, and the desired pure complex was extracted in the CH_2Cl_2 layer by solvent extraction. The CH_2Cl_2 layer was dried over anhydrous $MgSO_4$, and CH_2Cl_2 was removed to isolate the pure compounds **I**, **II**, and **III**. Yields for the respective desired complexes are typically 55—60% based on the reactants used. Elemental analysis data **(**obtained; calculated**)**: **I**: C 46.9, H 3.0, N 8.3, C 46.85, H 3.02, N 8.41. **II**: C 63.9, H 3.6, N 9.2, C 63.89, H 3.69, N 9.31. **III**: C 62.4, H 3.4, N 9.0, C 62.24, H 3.59, N 9.07. FAB mass data: **I** 668 (M^+) (15%), 523 (M^+-PF_6) (25%); **II** 1202 (M^+) (2%), 1059 (M^+-PF_6) (5%); **III** 1090 (M^+-PF_6) (2%). All complexes, **I**, **II** and **III**, were paramagnetic, and g_{av} evaluated (CH_2Cl_2; RT) for these complexes was with in the range 2.0016—2.0014.

(14) Boone, S. R.; Pierpont, C. G. *Inorg. Chem.* **1987**, *26*, 1769.

(15) Ramakrishna, G.; Singh, A. K.; Palit, D. K.; Ghosh, H. N. *J. Phys. Chem. B* **2004**, *108*, 1701.

(16) Woutersen, S.; Bakker, H. B. *Nature* **1999**, *402*, 507.

(17) Jarzeba, W.; Walker, G. C.; Johnson, A. E.; Michael, A. K.; Barbara, P. F. *J. Phys. Chem.* **1988**, *92*, 7039.

(18) Jarzeba, W.; Walker, G. C.; Johnson, A. E.; Barbara, P. F. *Chem. Phys.* **1991**, *152*, 57.

(19) (a) Pecourt, J.-M. L.; Peon, J.; Kohler, B. *J. Am. Chem. Soc.* **2000**, *122*, 9348. (b) Pecourt, J.-M. L.; Peon, J.; Kohler, B. *J. Am. Chem. Soc.* **2001**, *123*, 10370. (c) Ulrich, S.; Schultz, T.; Zgierski, M. Z.; Stolow, A. *J. Am. Chem. Soc.* **2004**, *125*, 2262. (d) Kime, N. J.; Jeong G.; Kim, Y. S.; Sung, J.; Kim, S. K.; Park, Y. D. J. *Chem. Phys.* **2000**, *113*, 10051.

(20) Fidder, H.; Rini, M.; Nibbering, E. T. *J. Am. Chem. Soc.* **2004**, *126*, 3789.